



Communication

# Application of depth-sensing microindentation testing to study of interfacial transition zone in reinforced concrete

Wenzhong Zhu\*, Peter J.M. Bartos

*Advanced Concrete and Masonry Centre, Department of Civil Engineering, University of Paisley, High Street, Paisley, Scotland PA1 2BE, UK*

Received 29 March 2000; accepted 6 June 2000

## Abstract

A new method, the depth-sensing microindentation technique, was successfully used to study the elastic modulus and micro-strength of the interfacial transition zone (ITZ) around steel reinforcement in practical reinforced concrete. A normal concrete mix and a special self-compacting concrete (SCC) mix, both produced commercially, were used in the study. It was found that the elastic modulus and microstrength in the ITZ were significantly lower on the bottom side of a horizontal steel reinforcement than on the top side. The difference was particularly pronounced in the 10–30  $\mu\text{m}$  distance from the actual interface. The method showed clear advantages over the conventional Vickers microhardness test. © 2000 Elsevier Science Ltd. All rights reserved.

**Keywords:** Interfacial transition zone; Micromechanics; Elastic moduli; High performance concrete

## 1. Introduction

The interfacial transition zone (ITZ) between cement paste and aggregate (or fibre) and around steel reinforcing bars has been an area of particular interest associated with engineering and durability properties of cementitious composites and structural reinforced concrete. As a result of its more porous and heterogeneous/anisotropic nature, the ITZ was recognised to be the ‘weak link’ in cement and concrete composites and to have a considerable influence on the engineering and durability properties. Recent development of special, high performance concrete, as well as various fibre-reinforced cementitious composites has further underlined the importance and urgent practical need in understanding and optimising the ITZ properties.

In a previous research [1], a unique depth-sensing microindentation method was successfully used for micro-strength testing and fibre push-in testing to assess interfacial and bond properties in glass fibre-reinforced cementitious composites. Significant advances have since

been made in improving the micro/nano-indentation test method and in theoretical analysis of the test data [2–4]. The depth-sensing microindentation method now offers great advantages over the conventional Vickers microhardness testing in three aspects. Firstly, apart from microhardness (or microstrength), the test can also provide well-defined mechanical parameters such as elastic modulus of the interfacial zone that can be used for modelling of the composites. Secondly, as load and depth of an indentation are continuously monitored, optical observation and measurement of diagonal length of the indent/impression, which can be difficult and subject to inaccuracy, is no longer required. Thirdly, instead of a fixed relatively flat Vickers indenter (depth being one-seventh of the diagonal length), different and sharper indenters can be used, so that the test area could be smaller but deeper. This is of great benefit to specimens obtained from practical composites where the valid test area available is relatively small as interference of different aggregates often exists, and specimens with surface irregularities which often present in the ITZ due to sample preparation.

In this study, the depth-sensing microindentation method was applied to investigate the ITZ in structural reinforced concrete, particularly the mechanical properties of the ITZ above and below a horizontal steel reinforcing bar. Two

\* Corresponding author. Tel.: +44-141-848-3758; fax: +44-141-848-3275.

E-mail address: wenzhong.zhu@paisley.ac.uk (W. Zhu).

types of concrete, a self-compacting concrete (SCC) mix and a normal concrete mix as reference, with characteristic cube strength of 60 MPa, were used for producing heavily reinforced beams. The SCC, being highly flowable and able to achieve adequate compaction under its own weight, was developed and used to facilitate the placement of concrete in structures with congested reinforcement. The SCC mix was poured into the formwork at one end, flowed and compacted in the 3.8-m beam by itself without vibration. Whereas the reference concrete (REF) was compacted conventionally into an identically reinforced beam using poker vibrators, thus providing a basis for comparison of ITZ properties in the two concretes.

## 2. Experimental

### 2.1. Concrete mixes used

Standard 42.5N grade Portland cement (Blue Circle), 10 mm maximum size granite aggregate, and medium grade sand were used as the basic materials for the concrete mixes. For the SCC mix a special admixture, provided by Sika, and granulated ground blastfurnace slag (GGBS), provided by Castle Cement, were also used. For the REF mix, a common superplasticiser was used. The concrete mixes were designed to strength grade of 60 MPa, and produced commercially at a local Ready Mix Concrete plant. Details of the mixes and properties are given in Table 1.

### 2.2. Element cast and specimen preparation

The identical beams for the two types of concrete were designed to comply with the requirement of Euro-code 2, with design load generating bending moment of  $M = 120$  kN m. Details of the reinforcement are given in Fig. 1. The formwork for the beams was stripped and

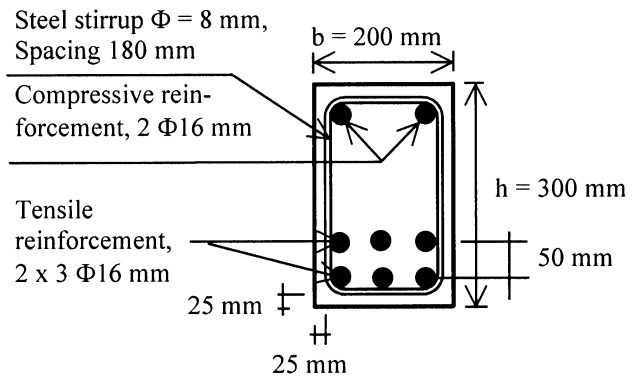


Fig. 1. Details of the reinforcement in  $200 \times 300 \times 3800$  mm beam.

the beams immediately sprayed with a curing compound at 6 days.

Specimen for the microindentation testing were prepared by first drilling  $\Phi 100 \times 200$  mm cores horizontally from the middle section of the beam, the cores intersecting the three  $\Phi 16$  reinforcing bars of the upper layer in the tensile zone. Small specimens (roughly  $\Phi 35 \times 20$  mm) with only one steel bar at the centre were then extracted from the cores taken, using a diamond saw. This was then followed by procedures [1] including resin embedding, precision sectioning, grinding, polishing and ultrasonic cleaning to obtain the final disc specimens ( $\Phi 40 \times 15$  mm) for the microindentation test.

### 2.3. Measurement of elastic modulus and microstrength

All experiments were performed using a depth-sensing microindentation apparatus, MicroTest 200, available at University of Paisley. The load and depth (or displacement of the indenter) were continuously monitored during a programmed microindentation load cycling. The operating principle and special features of the apparatus were described in detail elsewhere [1]. A relatively sharp  $90^\circ$  diamond indenter/probe in the shape of a corner of a cube was selected for this study so that smaller but deeper indentation could be made. This would also make the test results less sensitive to the surface effect (e.g. roughness and hardening/densification) due to imperfect specimen preparation.

A typical outcome of the microindentation testing is an indentation load-depth hysteresis curve as shown in Fig. 2. As a load is applied to an indenter in contact with a specimen surface, an indent/impression is produced that consists of permanent/plastic deformation and temporary/elastic deformation. Recovery of the elastic deformation occurs when unloading is started. Determination of the elastic recovery by analysing the unloading data according to a model for the elastic contact problem leads to a solution for calculation of elastic modulus  $E$  and also micro-strength/hardness  $H$  of the test area. Details of the theoretical background and methodology for the elastic

Table 1  
Details of the concrete mixes used

	SCC mix	Reference mix
<i>Mix proportions, kg/m<sup>3</sup></i>		
Portland cement, 42.5N	330	525
GGBS	200	—
Granite, 6–10 mm	750	950
Natural washed glacial sand	870	670
Admixture	5.3	6.4
Free water	192	225
<i>Basic concrete properties</i>		
Slump, mm	—	100
Slump flow, mm	650	—
Air content, %	1.5	1.8
Estimated in-situ compressive strength at 3 month, MPa <sup>a</sup>	66	60

<sup>a</sup> Obtained from cores using BS 1881: part 120: 1983.

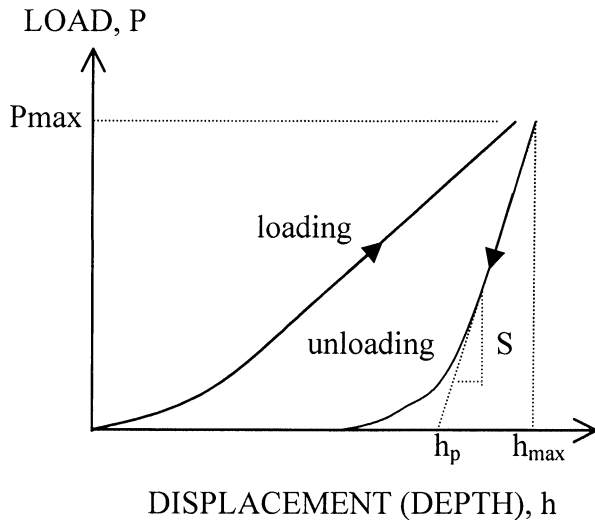


Fig. 2. A schematic diagram of an indentation load vs. displacement curve.

modulus determination have been reviewed and presented elsewhere [2,4].

Briefly, the specimen elastic modulus is determined using Eqs. (1) and (2):

$$S = \frac{dP}{dh} = \frac{2}{\sqrt{\pi}} E_r \sqrt{A}, \quad (1)$$

$$\frac{1}{E_r} = \frac{(1 - \nu^2)}{E} + \frac{(1 - \nu_i^2)}{E_i} \quad (2)$$

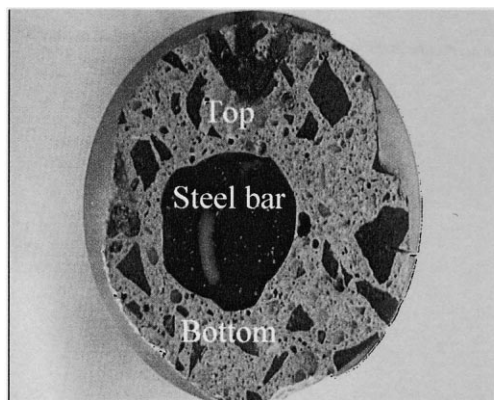
where  $S = dP/dh$  is the experimentally measured stiffness of the upper portion of the unloading data;  $E_r$  is a reduced elastic modulus defined in Eq. (2);  $A$  is the projected area of the elastic contact;  $E$  and  $\nu$  are Young's modulus and Poisson's ratio for the specimen; and  $E_i$  and  $\nu_i$  are the same parameters for the indenter. For the diamond indenter used in this study,  $E_i = 1141$  GPa and  $\nu = 0.07$ . The projected area  $A$  can be derived from the plastic depth  $h_p$  obtained using the unloading data and the indenter shape function, which is dependent on its geometry. For an ideally perfect

$90^\circ$  (corner of a cube) indenter,  $A = 2.6h_p^2$ . In the case of imperfect indenter tip geometry, the shape function can be determined by using electron microscopy techniques or through calibration of a hardness (or elastic modulus) — plastic depth curve using a homogeneous material of constant hardness (or elastic modulus). A special defined parameter — microstrength,  $H = P_{\max}/A$ , can also be calculated, where  $P_{\max}$  is the maximum load applied. When the Vickers indenter is used the microstrength is equivalent to the Vickers microhardness.

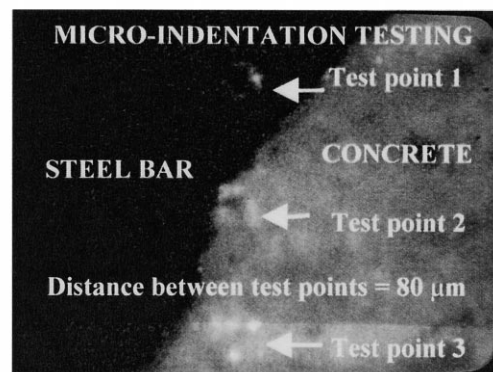
### 3. Results and discussions

In this study all testing was programmed in such a way that the loading started when the indenter came into contact with the test surface and the load increased at a constant rate of 2.3 m N/s until a depth of penetration of indenter into the specimen reached a specified value of 10  $\mu\text{m}$ . Then the load was held at its maximum for 10 s before unloading at the same constant rate. At completion of unloading, the specimen was retracted and moved to another test point. With the maximum depth setting of 10  $\mu\text{m}$  the width of the indent/impression after the load removal was usually about 20  $\mu\text{m}$  or less. The distance between two adjacent test points was thus set to be 60  $\mu\text{m}$  or greater, to avoid possible overlapping of the areas affected.

Photographs of a test specimen and a magnified tested interfacial area are shown in Fig. 3. To study the interfacial zone around the horizontal reinforcing bar in both SCC and conventional concrete mixes, a large number of indentation tests were carried out in the steel–concrete interfacial areas at the top and the bottom sides (i.e. above and below) of the steel bar. Since sand particles also existed in the tested area, the test points that lie closer to the aggregate particles than to the steel bar were considered invalid and discarded. A typical test of results is presented in Fig. 4 as plots of modulus of elasticity and microstrength versus distance from the interface.



(a)



(b)

Fig. 3. Photographs of the tested specimen: (a) specimen of the indentation test and (b) magnified view of interfacial area after testing.

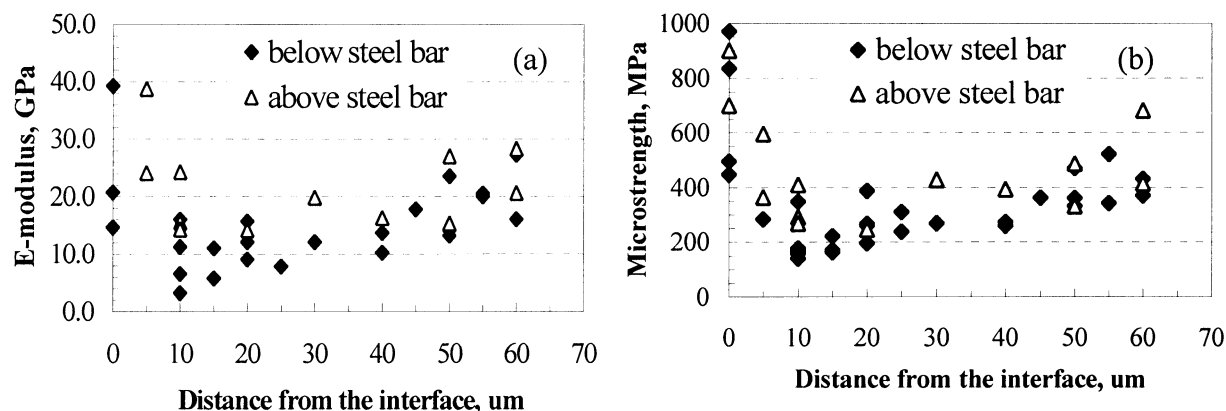


Fig. 4. A typical set of results versus distance from the interface for: (a) elastic modulus and (b) microstrength.

For all the specimens tested in this study, it was found that the micro-mechanical property (i.e. modulus and strength) profiles showed a trough within the ITZ, with the minimum values occurring at 10–30  $\mu\text{m}$  from the actual steel interface. The micro-mechanical properties then increased when test points moved towards the bulk concrete matrix and became roughly constant at distances greater than 50–70  $\mu\text{m}$ . It was also noted that the results showed moderate variations even at the same distance from the interface, and that interference of neighbouring aggregate/sand particles became more frequent at distances greater than 60  $\mu\text{m}$  from the steel interface. The interference of steel bar was also present for test points adjacent to or less than 10  $\mu\text{m}$  from the interface.

For comparison of the micro-mechanical properties of different test areas of the ITZ and evaluation of their variations, the test points were classified into two groups according to their distance  $d$  to the actual interface, namely 10  $\mu\text{m} < d < 30 \mu\text{m}$ , and 35  $\mu\text{m} < d < 60 \mu\text{m}$ . The results for the 10–30  $\mu\text{m}$  distance can be considered to represent the minimum value within the ITZ, whereas the results for the 35–60  $\mu\text{m}$  distance may provide an indication of properties of the bulk matrix. Average results and the standard deviations of modulus of elasticity and micro-strength for both

the SCC and reference mixes are presented in Table 2. The results of interfacial properties below steel bar relative to the above steel bar are presented in Fig. 5.

The results in Table 2 and Fig. 5 clearly indicate that the elastic modulus and microstrength of the ITZ were significantly lower on the bottom side of the steel bar than on the top side. The difference was particularly pronounced in the 10–30  $\mu\text{m}$  distance from the actual interface and for the reference mix. For instance, at the distance of 10–30  $\mu\text{m}$ , the interfacial  $E$  modulus and micro-strength below the steel bar was only 56% and 70%, respectively, of those above the bar for the reference mix. The corresponding results for the SCC mix were 86% and 69%, which seemed to suggest that the ITZ properties were more uniform in the SCC mix than in the reference mix. This may be due to the relatively lower water content and higher powder volume in the fresh SCC mix. The average results for the distance of 35–60  $\mu\text{m}$  from the interface showed that both properties on the bottom side achieved 80% of those on the top side for the reference mix, whereas for the SCC mix almost identical values were obtained on both sides. This was mainly due to the fact that for the reference mix the weak interfacial zone was found to be wider on the bottom side than on

Table 2  
Modulus of elasticity and micro-strength in the ITZ around steel bar

Properties	Reference mix (REF)		SCC mix (SCC)	
	Below steel bar	Above steel bar	Below steel bar	Above steel bar
<i>Modulus of elasticity, GPa</i>				
10 < $d$ < 30 $\mu\text{m}$	9.8	17.6	12.9	15.0
Standard deviation	4.0	4.4	4.5	5.5
35 < $d$ < 60 $\mu\text{m}$	17.6	21.5	25.2	24.4
Standard deviation	5.1	5.9	4.6	3.8
<i>Micro-strength, MPa</i>				
10 < $d$ < 30 $\mu\text{m}$	229	329	197	285
Standard deviation	77	84	46	74
35 < $d$ < 60 $\mu\text{m}$	372	462	411	418
Standard deviation	82	135	125	61

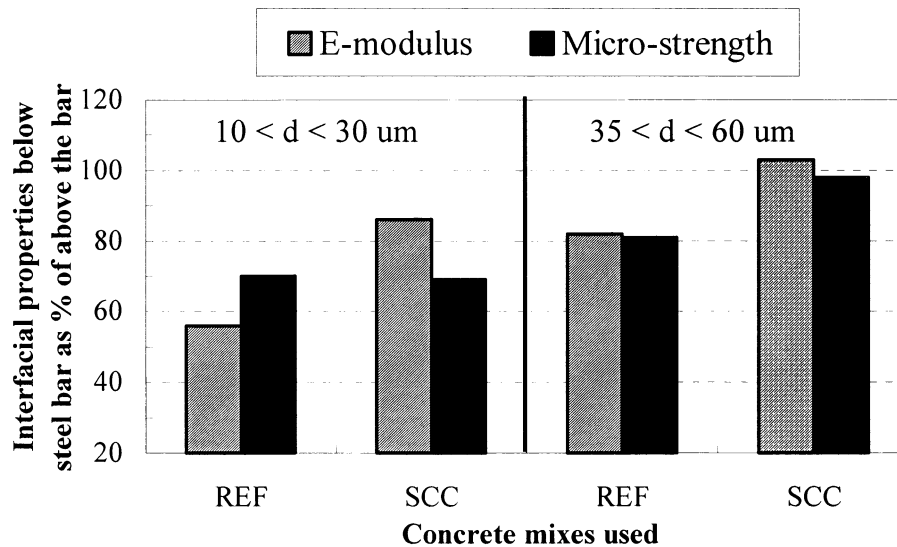


Fig. 5. Results of ITZ properties below steel bar relative to above steel bar, %.

the top side of the bar. Such a phenomenon was not evident in the SCC mix.

It should be stressed that in contrast to many previous studies where over-simplified model composite specimens were used [5–8], the specimens used in this study were extracted from real commercially produced structural concrete elements. This was achieved mainly with the use of the advanced depth-sensing micro-indentation method and the relatively sharp  $90^\circ$  indenter/probe. As a result the indentation area used was smaller but much deeper, compared to that of the Vickers microhardness testing. For instance, with the maximum indentation depth of  $10 \mu\text{m}$  adopted in this investigation the width of the indent was only about  $20 \mu\text{m}$ . Had the Vickers indenter been used, the average diagonal length of the indent for the same depth would have been over  $70 \mu\text{m}$ . The adoption of real specimen and the smaller but deeper indentation area, however, may also partly contribute to the moderate scatter of results observed in this study. This is because the interference of nearby aggregate/sand particles that lie underneath the polished surface could not be easily detected.

#### 4. Conclusions

The results and data used in this study were obtained during extensive pilot trials to evaluate the potential of using the depth-sensing microindentation method for determination of ITZ micro-mechanical properties in cementitious composites, and to assess the performance of SCC. Work currently in progress includes trials to further enhance the performance of the test apparatus and to study ITZ around steel reinforcement and coarse aggregate in other concrete mixes. The following conclusions can be drawn from the results obtained so far.

(1) A new method, the depth-sensing microindentation technique, was successfully used to study the elastic modulus and micro-strength of the ITZ around steel reinforcement in practical reinforced concrete. This method offers a clear advantage over the conventional Vickers microhardness test.

(2) The results obtained for both the SCC and the reference mixes revealed the distribution of micro-mechanical properties within ITZ which showed a common profile, namely with a trough or a minimum occurring at  $10\text{--}30 \mu\text{m}$  from the actual steel interface. The width of the ITZ was found to be between  $50$  and  $70 \mu\text{m}$  beyond which the micro-mechanical properties became less variable.

(3) The results indicated that the elastic modulus and the micro-strength of the ITZ were significantly lower on the bottom side of a horizontal steel reinforcement than on the top side. This supported the common perception that ITZ underneath a large aggregate particle or steel bar is weaker than above it, owing to internal bleeding and settlement of particles during concrete placing. This effect was particularly pronounced in the  $10\text{--}30 \mu\text{m}$  distance from the actual interface.

(4) The difference of ITZ properties between the top and bottom side of the horizontal steel bar seemed to be generally less pronounced for the SCC mix than for the reference mix.

#### References

- [1] W. Zhu, P.J.M. Bartos, Assessment of interfacial microstructure and bond properties in aged GRC using a novel microindentation method, *Cem Concr Res* 27 (1997) 1701–1711.
- [2] W.C. Oliver, G.M. Pharr, An improved technique for determining hardness and elastic modulus using load and displacement sensing indentation experiments, *J Mater Res* 7 (1992) 1564–1579.

- [3] M.F. Doerner, W.D. Nix, A method for interpreting the data from depth sensing indentation instruments, *J Mater Res* 1 (1986) 601–609.
- [4] P. Trtik, P.J.M. Bartos, Micromechanical properties of cementitious composites, *Mater Struct* 32 (1999) 388–393.
- [5] W. Sun, J.A. Mandel, S. Said, The effects of a new mixing technique on the properties of the cement paste–aggregate interface, *ACI J* 83 (1986) 597–605.
- [6] P.K. Mehta, P.J.M. Monteiro, Effect of aggregate, cement and mineral admixtures on the microstructure of the transition zone, in: S. Mindess, S. Shah (Eds.), *Proc Mater Res Soc Symp Vol. 114*, 1988, pp. 65–75.
- [7] A.K. Tamimi, The effects of a new mixing technique on the properties of the cement paste–aggregate interface, *Cem Concr Res* 24 (1994) 1299–1304.
- [8] S. Igarashi, A. Bentur, S. Mindess, Microhardness testing of cementitious materials, *Adv Cem Based Mater* 4 (1996) 48–57.